

Journal of Biomedical Optics

SPIEDigitalLibrary.org/jbo

Dynamic photopatterning of cells *in situ* by Q-switched neodymium-doped yttrium ortho-vanadate laser

Gitanjal Deka
Kazunori Okano
Fu-Jen Kao



SPIE

Dynamic photopatterning of cells *in situ* by Q-switched neodymium-doped yttrium ortho-vanadate laser

Gitanjal Deka,^a Kazunori Okano,^{a,b,c,d} and Fu-Jen Kao^a

^aNational Yang-Ming University, Institute of Biophotonics, Taipei, Taiwan

^bNational Chiao Tung University, Center for Interdisciplinary Science, Hsinchu, Taiwan

^cTohoku Fukushi University, Kansei Fukushi Research Institute, Sendai, Japan

^dNara Institute of Science and Technology, Ikoma, Japan

Abstract. Cellular micropatterning has been increasingly adopted in quantitative biological experiments. A Q-switched pulsed neodymium-doped yttrium ortho-vanadate (Nd:YVO₄) laser directed *in-situ* microfabrication technique for cell patterning is presented. A platform is designed uniquely to achieve laser ablation. The platform is comprised of thin gold coating over a glass surface that functions as a thermal transducer and is over-layered by a cell repellent polymer layer. Micropatterns are engraved on the platform, subsequently exposing specific cell adhesive micro-domains by ablating the gold-polymer coating photothermally. Experimental results indicate that the proposed approach is applicable under culture conditions, viable toward cells, and has a higher engraving speed. Possible uses in arraying isolated single cells on the platform are also shown. Additionally, based on those micro-patterns, dynamic cellular morphological changes and migrational speed in response to geometrical barriers are studied to demonstrate the potential applications of the proposed approach. Our results further demonstrate that cells in narrower geometry had elongated shapes and higher migrational speed than those in wider geometry. Importantly, the proposed approach will provide a valuable reference for efforts to study single cell dynamics and cellular migration related processes for areas such as cell division, wound healing, and cancer invasion. © The Authors. Published by SPIE under a Creative Commons Attribution 3.0 Unported License. Distribution or reproduction of this work in whole or in part requires full attribution of the original publication, including its DOI. [DOI: [10.1117/1.JBO.19.1.011012](https://doi.org/10.1117/1.JBO.19.1.011012)]

Keywords: laser ablation; thermal transducer; cytophobic polymer; cell array; cellular migration.

Paper 130185SSR received Mar. 29, 2013; revised manuscript received Jul. 12, 2013; accepted for publication Jul. 23, 2013; published online Aug. 19, 2013.

1 Introduction

Cell culturing is essential for biological examination in life sciences and clinical biochemistry. Cellular micropatterning has been used in cellular analyses,¹⁻³ cell based sensing and drug testing,⁴⁻⁶ tissue engineering,⁷ and specific cell-cell interaction studies.³ To acquire precise cellular information, researchers culture individual cells by using microfabrication techniques.^{8,9} Fabricating micro-culture devices involves developing specific cell adhesive areas on a solid platform.¹ In practice, cell patterning is achieved by using microculture devices that are prefabricated by photolithography,¹⁰ soft lithography,¹¹ and micro-contact-printing.¹² Despite growing on those micro-devices and connect with each other through prefabricated patterns, use of this approaches may be inadequate for some applications in cytological study, since living cells divide, differentiate, and migrate. For specific requirements, the prepared platform patterns may need to be altered dynamically to form cell-cell interactions while cells are growing. The dynamic control of cell adhesive activity on solid surfaces has received considerable attention.^{1,13} Related studies have used electrochemically reactive,¹⁴⁻¹⁶ photoactive,^{17,18} enzymatically reactive,¹⁹ and thermally responsive platforms,²⁰⁻²² capable of altering the cell adhesiveness dynamically.

Position specific removal of surface materials by using lasers to array biomolecules and cells is an emerging approach in

quantitative biomedical study.^{23,24} Using a laser is advantageous in that it affects only the local area. Moriguchi et al. presented an approach that uses Nd:YAG laser induced photothermal ablation to connect cells between two prefabricated domains.²⁵ Although that approach used chromium as the thermal transducer layer, its toxicity toward cells makes it inadequate for dynamic biological applications. Additionally, that approach could not form the entire domain for cell attachment; instead it made a tunnel for cell connections at the bottom of the thick agaros layer. Agaros is further limited by its instability and high bacterial affinity.²⁶ Previously our group developed a femto-second laser induced *in-situ* micro-fabrication method to array cells on a platform with micrometer-scale cell-adhering domains on a cytophobic surface under culture conditions.^{27,28} The method was based on photochemical ablation.²⁸ In terms of promoting the use of *in-situ* lithography in biological research, frequent tuning requirements and high costs of the femto-second laser are prohibitive. Additionally, the engraving speed of Ti:sapphire is only around 20 $\mu\text{m/s}$ with a pulse frequency of 1 kHz,²⁷ which is too slow to make a pattern in a platform of 3 to 4 cm^2 .

This work presents a novel dynamic *in-situ* ablation method for photopatterning of cells in a specially designed platform. Ablation by neodymium-doped yttrium ortho-vanadate (Nd:YVO₄) laser was markedly faster (i.e., 800 mm/s) than that of Ti:sapphire, making it suitable to achieve *in-situ* alteration of the platform patterns to study dynamics of cells in an array. *In vitro* monitoring of collective cell migration speed was also performed in response to geometrical barriers.

Address all correspondence to: Fu-Jen Kao, National Yang-Ming University, Institute of Biophotonics, 155, Linong Street, Section 2, Taipei 11221, Taiwan. Tel: +886-2-28267336; Fax: +886-2-28235460; E-mail: fjkao@ym.edu.tw

Additionally, morphological changes in the growing cells against the width of the pattern were examined. Moreover, cell survivability at different distances of laser irradiation was studied using an array of HeLa cells. Importantly, this work develops a highly promising microfabrication method for quantitative analysis of cellular processes such as cell division, cell morphology, and migration for biomedical studies.

2 Materials and Methods

2.1 Fabrication of Cell Array Platform

The cell array platform was fabricated by coating a glass plate with a thin layer of platinum and gold sequentially. The 30-nm gold coating was achieved by physical vapor deposition in an electron beam evaporation system. Before that, the same glass slide was over-layered by an extremely thin 7-nm platinum layer to achieve a satisfactory attachment of gold particles. The gold layer over the substrate functioned as the thermal transducer layer to achieve proper photothermal ablation. Next, a cytophobic layer was formed over the transducer layer by soaking the substrate in a 0.2% (w/v) solution of 2-methacryloxyethyl phosphorylcholine (MPC) polymer in ethanol. Upon drying, the substrate was ready for use. When the laser was focused, the transducer layer absorbed light energy and produce a local heat of high degree at the laser spot. At a rather high temperature, the cytophobic polymer and transducer layers were depleted, subsequently exposing the cytophilic glass layer.

2.2 Experimental Setup

The setup of the laser micro-engraving system consists of a diode-pumped Q-switched Nd:YVO₄ laser, piloting diode laser, pair of scanning galvano meter mirrors, and water immersion objective lens with a numerical aperture (NA) of 0.3 [Fig. 1(a)]. Central wavelength of the Q-switched laser is 1064 nm, with a peak power of around 220 mW. The Nd:YVO₄ laser beam was focused on the transducer layer under the

guidance of the piloting diode laser of wavelength 653 nm through a 10× water-immersing objective (Olympus, Japan) coupled in a modified Olympus microscope system (Olympus, Japan) [Fig. 1(a)]. The maximum detectable laser power was 120 mW at the focal plane. Based on a computer control by marking mate, laser marking software, the laser beam was vector scanned for pattern drawing by galvano mirrors [Fig. 1(a)]. The patterns were designed on computer graphics as typically shown in Fig. 1(b), where 136 circles (20 μm) are written.

2.3 Cell Culture

Cervical carcinoma HeLa cells were cultured in Dulbecco's modified eagle medium supplemented with 10% fetal bovine serum, streptomycin, and penicillin. Next, cells were seeded on the substrates with a concentration of 2000 cells/cm². Culturing was performed in humidified atmosphere at 37°C with 5% CO₂.²⁹ For further dynamic alteration of cell adhesiveness, the laser was carefully irradiated on the substrate at a safe distance from the preresiding cells to prevent cell damage.

2.4 Cell Observation

Cells on the respective micro-domains were observed under a normal wide field microscope (Olympus, Japan) with 20× objective of NA 0.4. The images were taken with an Olympus digital camera "Camedia C-5060" (Olympus, Japan) that is compatible with the microscope.

3 Results

3.1 Photothermal Engraving

Cell cultivation micro-domains were fabricated through photothermal ablation by area specific removal of the MPC polymer by spot heating with a focused laser beam on a thin light-absorbing gold layer. Owing to that the polymer fails to absorb light at 1064 nm; the gold coating over the glass substrate functions as a

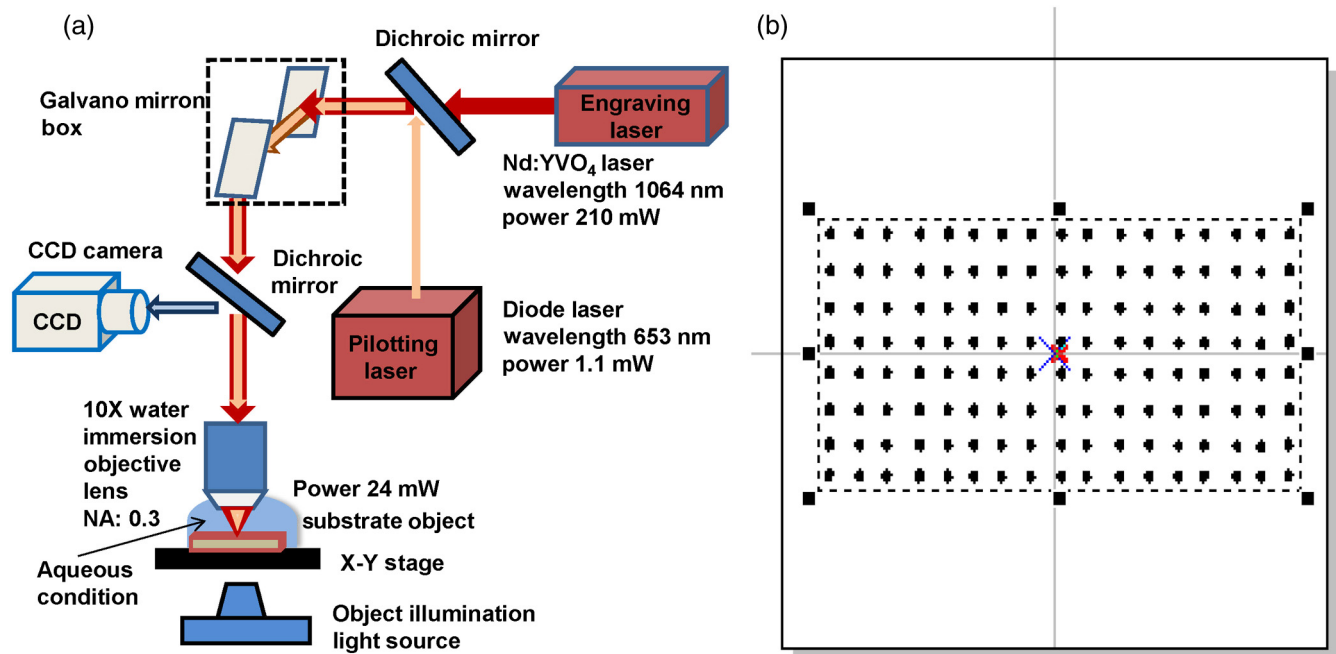


Fig. 1 Laser engraving system for biological applications: (a) schematic and (b) circular array patterns of the laser marking system.

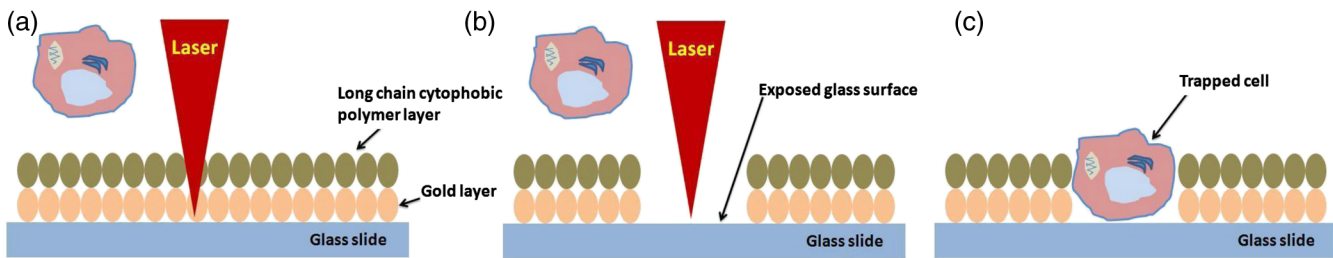


Fig. 2 (a and b) Schematic diagram of the cell adhesiveness alteration of the platform by photothermal ablation. (c) Trapped cell in cell adhesive domain.

photothermal transducer that transforms light energy into heat. The cytophobic MPC polymer film along with the underneath gold layer ablated at the laser spot exposing the cell-adhering domains. Figure 2 schematically depicts the cell adhesiveness alteration. This work first designed an array of desired pattern *in silico*, which functioned as the mold for the pattern engraving. Those patterns were engraved on the platform by the focused Nd:YVO₄ laser. The laser scanning speed and frequency were controlled through a pair of scanning galvano mirrors, with a computer system. In this work, two micropatterns were engraved: one was an array of circular domains, each with a diameter of 20 μm . The other one was rectangular, with a length of 1 mm and breadth of 150 μm . Figure 3(a) and 3(b) shows the circular array and rectangular microdomains, respectively, before and after cell seeding.

Experimental results indicated that the ablation in an aqueous condition was more confined than that of air for the same applied laser power. Figure 4(a) displays the scatter plot of

the pattern width dependency on laser power and environmental conditions, indicating that the ablation was feasible above 5 mW laser power for both air and water conditions. Upon increase in power, the size of the ablated area increased and, at one point, reached saturation value. For engraving under an aqueous condition, 10 mW was the saturation power above which the pattern sizes remained at 20 μm . Conversely, in air, the saturated size of 30 μm was measured at 35 mW power. To better determine the laser substrate interaction, we used two different concentrations of MPC polymer 0.1% and 0.05% in alcohol to compare the size of the ablated domain with the substrate without the polymer layer when the gold coating was 30-nm thick. Figure 4(b) depicts the scatter plots of the domain size (in diameter) of the engraved pattern in response to different MPC concentration for the same applied laser power. Experimental results show that without the polymer layer, the engraved domains have larger size than that in polymer layered substrates. However, the variation in polymer concentration did not cause detectable differences in domain size. We used gold layers of two different thicknesses, 30 and 50 nm, over-layered with 0.1% MPC polymer. The results indicate that laser ablates a larger area in 50-nm gold-coated surface than the 30 nm one for the same applied laser power. Figure 4(c) depicts the scatter plots of power against the diameter of the engraved domains for the two different thicknesses. This is attributed to the increase in light absorption due to deeper thickness.

The surface analysis of the laser engraved domain, in comparison to the unablated surface, was carried out by an atomic force microscope (AFM) and scanning electron microscope (SEM) (Fig. 5). Analysis of the results indicated that the ablated domain become rougher than the unablated gold MPC-coated surface that was observed by the pillars of the AFM histogram inside the engraved domain [Fig. 5(a)]. When the gold only coated surface was ablated, the number of pillars was less [Fig. 5(b)]. Figure 5(c) is the SEM image of the laser engraved area, where the bright area was the unablated region, rich in metallic gold, which gives bright a SEM image due to secondary electrons, in contrast to the dark area that lacks gold after ablation. Higher pillars were formed at the edge surrounding the engraved domain, which may be attributed to the folding of the polymer-coated gold layer as observed from the SEM image in Fig. 5(c). Some bright spots were observed inside the engraved region due to the presence of gold debris. A previous report suggests that a rough gold surface makes a better cell adherent platform than a smooth one.³⁰

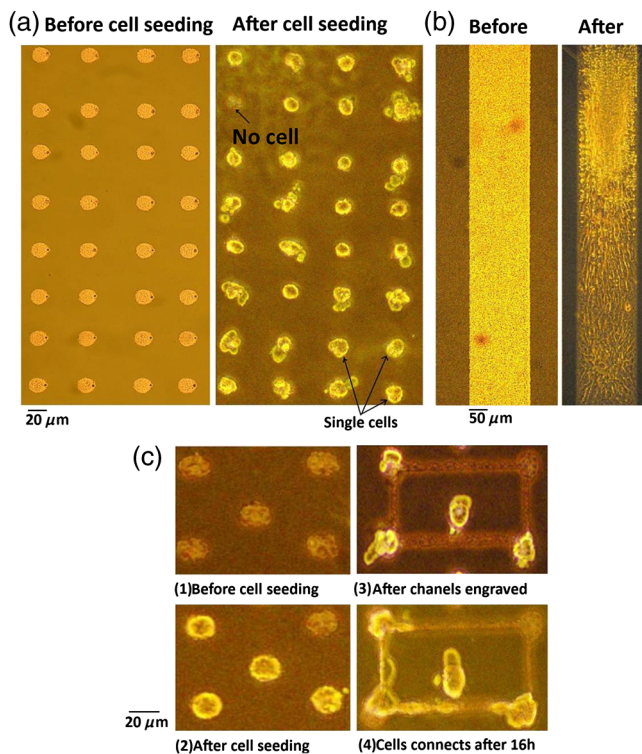


Fig. 3 Micrograph of the laser engraved area on the platform before and after cell seeding: (a) Single cells array in circular microdomains, (b) rectangular microdomain, and (c) connection induction along with the guided patterns.

3.2 Cell Array

For single cell cultivation, HeLa cells were seeded over the micropatterns. This work attempted to achieve a higher number

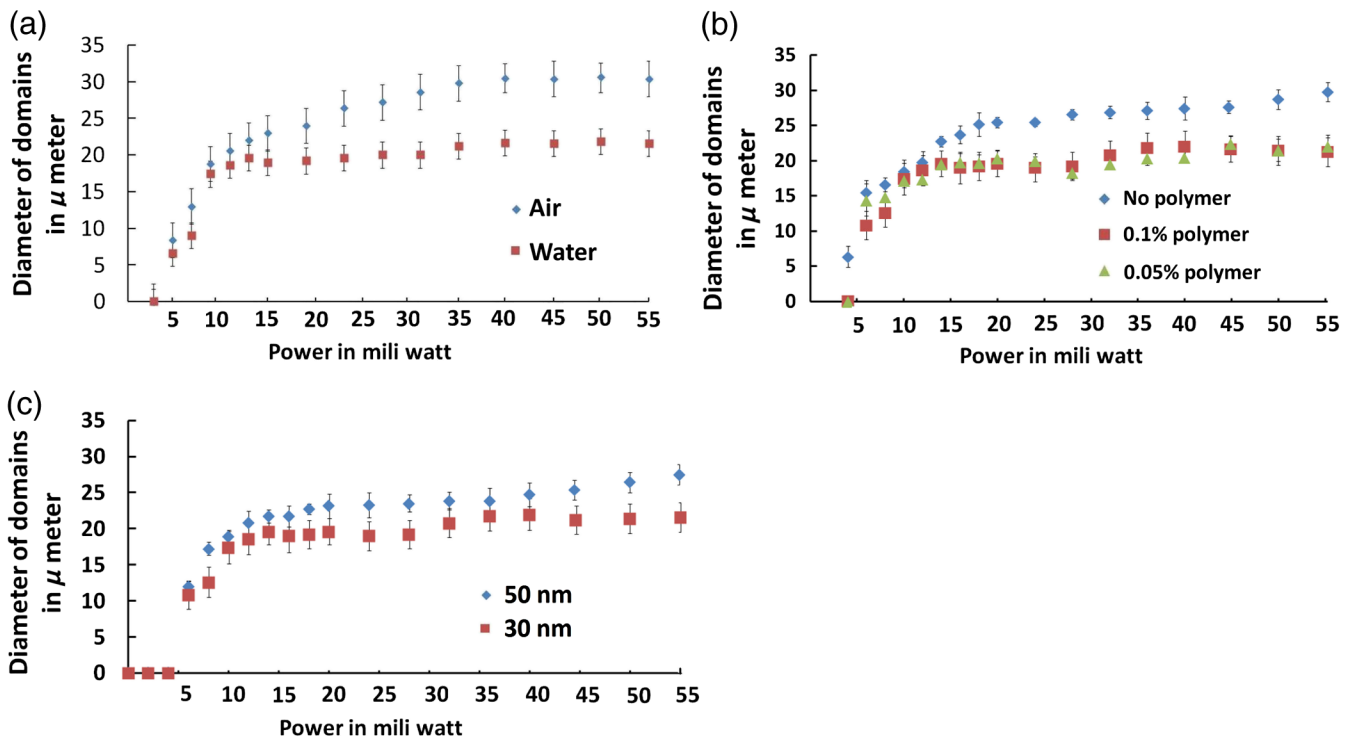


Fig. 4 Scatter plots of microdomain diameter as a function of the applied laser power. (a) The substrates were coated with 30-nm gold layer and over-layered by 0.1% MPC polymer. The difference is attributed to variation of thermal mass in air and water, respectively. (b) Comparison of no polymer over-layer and different concentrations of the MPC polymer over-layer under water. The substrate was coated with 30-nm thick gold layer. The polymer over-layer helps to contain the gold coating under ablation. (c) The effects due to different thickness of gold coating over-layered with 0.1% MPC polymer under water. Thicker coating would result in higher absorption and thus larger domain size. The error bars denote the standard error of the mean in diameter measurements.

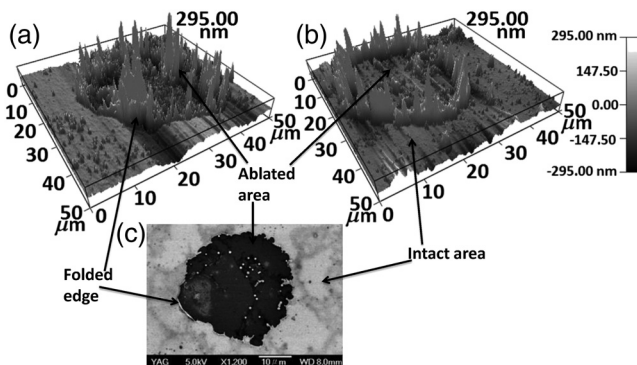


Fig. 5 Atomic force microscopy (AFM) and scanning electron microscopy (SEM) surface analysis of laser ablated domain. (a) AFM image of the ablated MPC-gold composite coated domain. (b) AFM image of the ablated gold-coated domain. (c) SEM image of the ablated MPC-gold composite-coated domain.

of single cells in a single domain by seeding highly disperse cells with a concentration of 3000 cells/cm². Comparable size of the microdomains with the cells was preferred for obtaining isolated single-cell culture. According to our results, not all the microdomains accommodated a single cell; it could occasionally have more than one cell and a few microdomains occasionally remained empty. Figure 3(a) shows such an array with single cells and empty microdomains denoted by arrows. To induce a cell-to-cell junction on the platform dynamically, engraving was performed *in situ* under culturing. Channels

connecting the microdomains were engraved without affecting the pre-existing cells.

After the cells were cultured for 24 h on the microdomains, the polymer layer between the domains was ablated to form channels of width around 10 μm . The cultured HeLa cells elongated along with the guided channels and connected to each other within 16 h. Figure 3(c) shows the engraved channel and cell-to-cell connection.

For quantitative analysis of single cell accommodation in response to different domain size, we have engraved patterns of three different diameters. If the domain size is approximately 15 μm or less in diameter, a higher percentage of the domains remain empty after cell seeding. In a selected area, only 21% of the domains contain cells; among them 78% are single cells. We have chosen 15 μm as the smallest domain to grow cells, since our method cannot create uniformly circular domains with diameters in the order of 10 μm . For domains of 20 μm diameter, 88% of the domains contain cells, with 43% of them being single cells. For even larger sized domains around 25 μm , 97% of domains are occupied by cells, with 16% of them single cells. Figure 6 shows cells growing on patterns of three different domains.

3.3 Effect of Laser Irradiation on a Cultured Cell

In-situ application of the laser was essential for the dynamic alteration of cell adhesiveness of the platform. Laser applications occasionally cause hypertrophy of the cells and can damage the cell if the laser focal spot is too close to the cell.^{27,31} Usually, application of an IR laser reduces the probability of

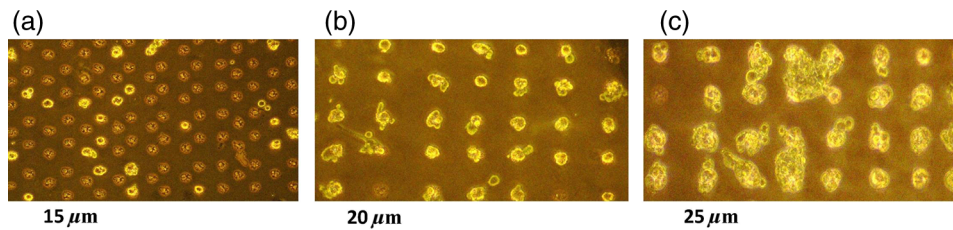


Fig. 6 Micrograph of cells in domains of diameter: (a) 15 μm , (b) 20 μm , and (c) 25 μm .

cell damage in comparison with using the UV laser.^{32–34} However, during *in-situ* engraving, the safe distance between the laser spot and the pre-existing cells had to be ensured. This study examined how the laser affects the cells, in which the percentage of damaged cells for different distances of the laser spot from the cells was evaluated. Figure 7(a) shows the laser spots along with the preexisting cells at different distances starting from 300, 200, 100, 50, and 0 μm (0 μm : laser application directly over the cell). Figure 7(b) illustrates the bar chart diagram of the percentage of cells after the laser irradiation at different distances. According to this figure, >80% of the cells survived after 24 h of the laser irradiation unless the laser was directly irradiated on the cells. Upon direct exposition to laser, only 40% of the cells stood in their respective cell adhesive domains after 24 h.

3.4 Cellular Migrational and Morphological Evaluation in Response to Geometrical Constraints

Cellular movement and their collective migration have received considerable interest in some of the physiological and biological processes, including embryonic development,³⁵ tissue morphogenesis,³⁶ wound healing,³⁷ and cancer metastasis.^{38,39} Their approach lacked a dynamic *in-situ* micro-fabrication method. Depending on the individual physiological requirements, cells can move as a wide sheet for wound closing and may travel in a narrow strip for cancer metastasis.⁴⁰ Here, a cell adhesive microdomain of width 150 μm and length 1 mm was fabricated on the nonadhesive substrate. Size and shape of the wound and the cancer thus have controlling effects in cellular migrational speed and modes.^{37,38} This study elucidates the role of geometrical constraint on collective cell migration by designing an *in vitro* assay using the proposed microfabrication approach based on the results of Vedula et al. on collective cell migration.⁴⁰

Their approach lacked a dynamic *in-situ* micro-fabrication method. The approach used in this study did not use external guiding biomolecules, such as fibronectin or collagen. Here, a cell adhesive microdomain of width 150 μm and length 10 mm was fabricated on the nonadhesive substrate. Figure 3(b) depicts one typical domain before and after cell seeding. HeLa cells were seeded and a mono layer was cultured for 2 days. Once the domain was filled with cells, strips were engraved with three different widths: 150, 100, and 50 μm , each with a length of 550 μm [Fig. 8(a)]. Consequently, a confluent monolayer of cells was grown in the reservoir, which was ready to flow through three guided strips. Figure 8(a) shows the confluent and its branched strips immediately after the formation of the strips; meanwhile, cells were grown inside the main microdomain. Some observable debris of dead cells and loosely attached cells were observed on the nonadhesive region, which disappeared after 2 to 3 days of culturing. Figure 8(b) displays typical micrographs of cellular migrational assay at an instance after 32 h of confluent formation. Analysis results indicated a faster cell sheet movement in a narrower strip than in the wider strips [Fig. 8(c)]. This finding complies with the same order of migration noted by Vedula et al.⁴⁰

Cellular migration can also affect the cell shape and morphology.⁴¹ Three rectangular microdomains were engraved with different widths of 150, 60, and 30 μm , to further elucidate the change in cellular morphology in relation to geometrical constraints. More elongated cells were observed along the length of the narrow domains, while the cells in the wider domains were less elongated (Fig. 9). Here, the ratio of cell length to breadth was defined as the parameter “cell shape factor” ($\beta = L/B$). The cell shape factor (β) at different microdomains was quantified and compared with cells in a normal culture dish (defined as microdomain with a width of α μm) in the bar chart diagram of Fig. 9(b). According to our results,

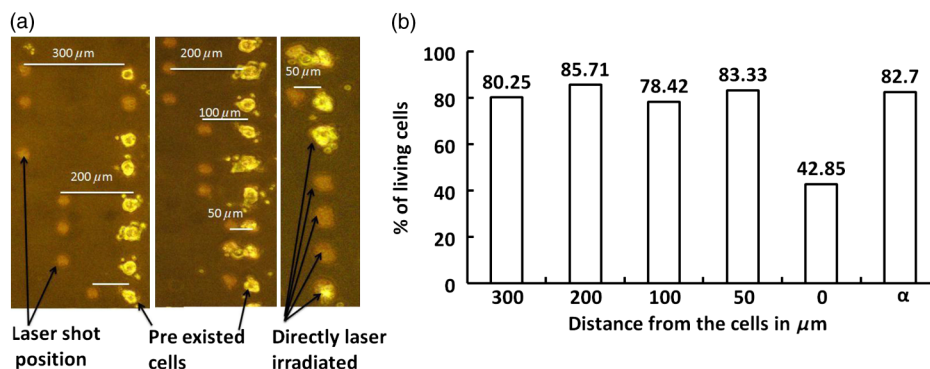


Fig. 7 (a) Micrograph of cells in their respective microdomains after 24 h since laser was irradiation at different distances. (b) Bar chart diagram of cell survivability study showing the percentage of cells lived after 24 h, in which the laser was irradiated at different positions tested for 30 cells each, where “ α ” denotes laser irradiation at an infinite distance from the cells.

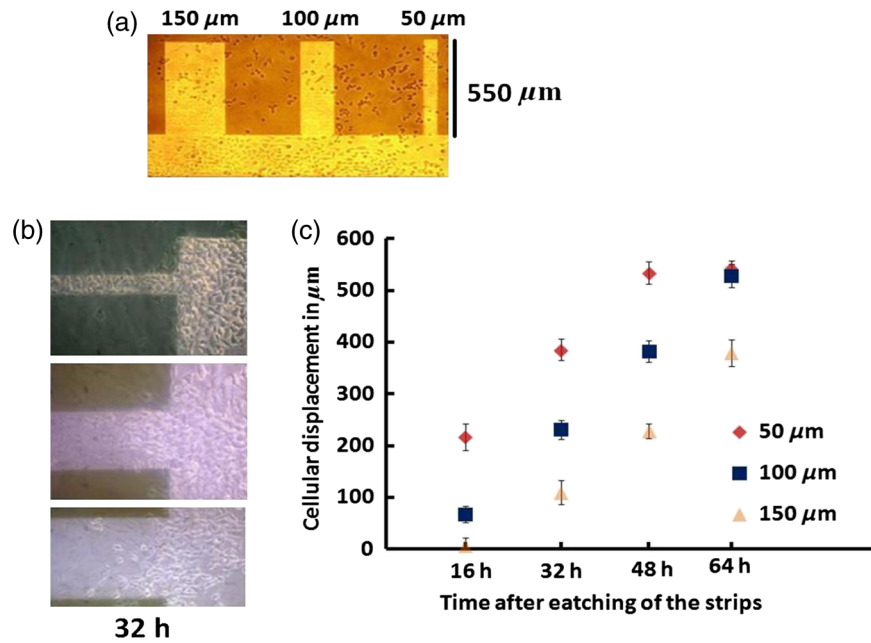


Fig. 8 (a) Representative image of a typical confluent monolayer with the guided strips immediately after formation. (b) Micrograph of the cellular displacement at an instant after 32 h of confluent formation. (c) Scatter plot of the cellular displacement assay through the strips. The error bars denote the standard error of the mean for cellular displacement measurements.

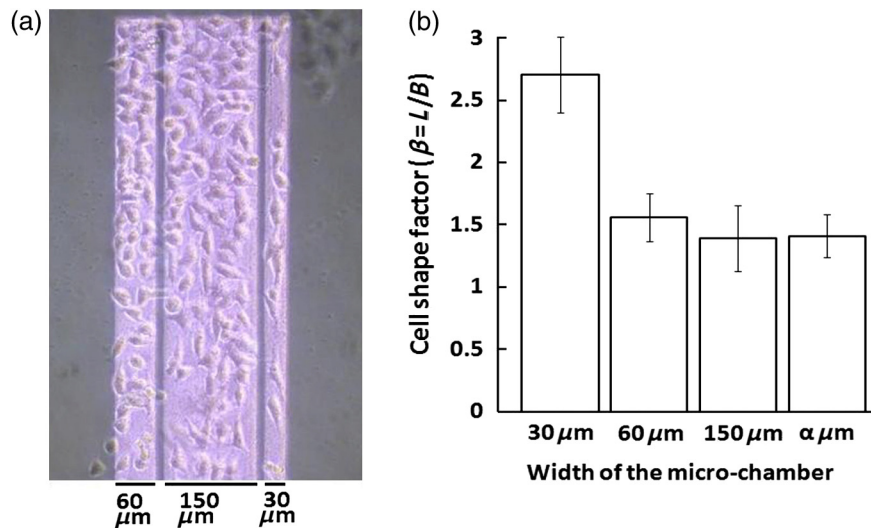


Fig. 9 (a) Photograph of the cells with different morphologies in domains with different geometrical configurations. (b) Bar chart diagram of cell shape factor ($\beta = L/B$) for the cells at different geometrical constraints. The error bar denotes the standard error of mean for β value measurements.

cells in wider domains have a similar size and shape with those in an open culture. The β value of cells in wider domains and normal culture dish was found to be around 1.4, whereas when the domain width was comparable to the cell size, cells took an elongated shape along the length of the domain (where $\beta = 2.7$).

4 Discussions

The approach adopted in this work is based on photothermal ablation phenomena. The gold transducer layer used in the platform plays a prominent role in the use of Nd:YVO₄ laser. This diode pumped laser was operated in Q-switch mode with nanosecond pulse width. However, this laser failed to induce photochemical ablation of used MPC polymer alone, whereas Ti:sapphire laser could.²⁷ Used gold coating absorbed laser photons

induced a thermal effect to ablate the over-layered cytophobic MPC polymer. This work developed an *in-situ* engraving approach, which was easy to handle, faster in operation, and cost effective. Since, the engraved width is 20 μm as shown in Fig. 3, the pulse interval of <20 μs is required. Nd:YVO₄ laser can thus engrave at a frequency 40 kHz with a speed of 800 mm/s, while Ti:sapphire engraves at 1 kHz with a speed of 20 μm/s.²⁷ Additionally, IR lasers are superior to UV lasers in biological applications, owing to the UV's risk factor toward cells.^{42,43}

Micro-fabricated cell array devices are in high demand owing to their importance in cell-to-cell interaction, drug testing, and neuronal signaling study.⁴⁴⁻⁴⁸ In this study, HeLa cells in specific micro-domains were cultured to demonstrate the

feasibility of a fabricated microculture platform in cell patterning. Due to the exposed glass surface surrounded by the non-adhesive areas, cells grew in geometrical microtraps. An array of single individual cells is beneficial in understanding the mechanism and function of each cell in detail. A notable example is the study of nerve cell interaction and time-dependent behavior of a cell during the division cycle.^{49–51} Additionally, this work demonstrated the possibility of cell-to-cell connections through the guided patterns, which can potentially be used for a quantitative neuronal signaling study.⁴⁷ For dynamic alteration of cell adhesiveness, we had to engrave patterns *in situ* under culture medium. Keeping this in mind, this work evaluated the size of the engraved areas in response to applied laser power under air and water environments. The smaller width of the patterns observed while engraving under water conditions was most likely owing to greater heat dissipation in water. However, engraving in air spreads the heat to a larger area, creating larger domains for the same applied laser power. This work also evaluates the effect of polymer layer on laser ablation. The polymer layer likely increases the binding of gold particles over the glass surface, acting as net-like adhesive. Thus, the ablated domain was larger when the gold coating was not over-layered with MPC polymer. Additionally, when the thickness of the gold coating increases, the absorption of photons increases as well, and this causes higher domain size than in the thinner gold layer. Figure 7 illustrates the effect of laser irradiation on the nearby cells. According to our results, 20% of the cells disappeared when the laser was applied away from the cell body, which was comparable with the value when the laser was focused at an infinite distance from the cells. We thus believed that the cell disappearance was due to normal cellular processes. However, for direct laser irradiation, focusing the laser partially on the gold coating along with the cell body might cause cell detachment. Conversely, a situation in which the laser beam had passed only through the cell body might not produce a heating effect; subsequently, the cell remained attached to the platform.

This work further demonstrated the applicability of the proposed micro-array platform in order to shed light on an important topic in biology: collective cell migration. Correspondingly, a confluent movement of cell collections through different strips was evaluated. Our results further illustrate that cells in narrow domains had elongated and aligned morphology in response to geometrical constraints. Differences in morphologies and alignment encouraged cells in wider strips to migrate in any direction, subsequently affecting their collective migration. Conversely, cells in the narrow strip tended to move only in one direction, which provided them higher migrational speed. We recommend further quantitative monitoring of cellular energy metabolism and effect of drugs in cell migration with the use of reported microculture platform in future.

5 Summary

This work has developed a novel cellular photopatterning approach. The proposed approach involved fabricating a unique cell arraying platform by coating gold thermal transducers on a cytophilic glass substrate, over-layered by cytophobic MPC polymer. Nd:YVO₄ laser ablative engraving of cell adhesive domains was then performed *in situ* on the platform. HeLa cells were cultured on the platform and found mainly growing in the cell adhesive domains. This work also investigated how

laser irradiation affected cells. Experimental results indicated that cells remained alive if the laser was not directly applied. This work further demonstrated the feasibility of growing individual cells and their ability to connect along a desired direction through guided channels. These platforms were also used to study the difference in cell migrational speed in response to geometrical constraints. Moreover, higher migrational speed and elongated cellular morphologies were observed in narrower domains than in wider domains. According to our results, Q-switch laser can be useful in cellular photopatterning. Importantly, the proposed approach is highly promising for use in a biomedical lab-on-a-chip study of quantitative biological processes that involves cells.

Acknowledgments

The authors would like to thank the National Science Council of the Republic of China, Taiwan and the “Aim for Top University” project of the Ministry of Education of the Republic of China, Taiwan for financially supporting this research. This study was partly supported by a program funding basic research centers in a private university from the Ministry of Education, Culture, Sports, Science, and Technology (MEXT) of Japan to the Kansei Fukushi Research Institute, Tohoku Fukushi University (2008 to 2012). Authors also show their gratitude to professor How-Foo Chen, associate professor, Institute of Biophotonics National Yang Ming University, for his kind help in fabricating the gold-coated glasses. Additionally, they also appreciate the kind gift of MPC polymer by Dr. Akio Hayashi of the NOF Corporation Japan. Dr. Po-Yen Lin, research fellow, Institute of Physics, Academia sinica, is appreciated for his kind help in acquiring the AFM images. Ted Knoy is appreciated for his editorial assistance.

References

1. J. Nakanishi et al., “Recent advances in cell micropatterning techniques for bioanalytical and biomedical sciences,” *Anal. Sci.* **24**(1), 67–72 (2008).
2. M. Nishizawa et al., “Micropatterning of HeLa cells on glass substrates and evaluation of respiratory activity using microelectrodes,” *Langmuir* **18**(9), 3645–3649 (2002).
3. D. Kleinfeld et al., “Controlled outgrowth of dissociated neurons on patterned substrates,” *J. Neurosci.* **8**(11), 4098–4120 (1988).
4. K. Bhadriraju and C. S. Chen, “Engineering cellular microenvironments to improve cell-based drug testing,” *Drug Discov. Today* **7**(11), 612–620 (2002).
5. D. Falconnet et al., “Surface engineering approaches to micropattern surfaces for cell-based assays,” *Biomaterials* **27**(16), 3044–3063 (2006).
6. R. Kapur et al., “Streamlining the drug discovery process by integrating miniaturization, high throughput screening, high content screening, and automation on the cellchip™ system,” *Biomed. Microdevices* **2**(2), 99–109 (1999).
7. H. Otsuka et al., “Two-dimensional multiarray formation of hepatocyte spheroids on a microfabricated PEG-Brush surface,” *Chembiochem* **5**(6), 850–855 (2004).
8. K. Yasuda, “On-chip single-cell-based microcultivation method for analysis of genetic information and epigenetic correlation of cells,” *J. Mol. Recognit.* **17**(3), 186–193 (2004).
9. A. Khademhosseini et al., “Layer-by-layer deposition of hyaluronic acid and poly-L-lysine for patterned cell co-cultures,” *Biomaterials* **25**(17), 3583–3592 (2004).
10. W. He et al., “Lithography application of a novel photoresist for patterning of cells,” *Biomaterials* **25**(11), 2055–2063 (2004).
11. Y. Xia and G. M. Whitesides, “Soft lithography,” *Angew. Chem., Int. Ed. Engl.* **37**(5), 551–575 (1998).

12. S. Zhang et al., "Biological surface engineering: a simple system for cell pattern formation," *Biomaterials* **20**(13), 1213–1220 (1999).
13. M. Yamato et al., "Thermally responsive polymer-grafted surfaces facilitate patterned cell seeding and co-culture," *Biomaterials* **23**(2), 561–567 (2002).
14. M. N. Yousaf et al., "Using electroactive substrates to pattern the attachment of two different cell populations," *Proc. Natl. Acad. Sci. U.S.A.* **98**(11), 5992–5996 (2001).
15. W. S. Yeo et al., "Dynamic interfaces between cells and surfaces: electroactive substrates that sequentially release and attach cells," *J. Am. Chem. Soc.* **125**(49), 14994–14995 (2003).
16. W. S. Dillmore et al., "A photochemical method for patterning the immobilization of ligands and cells to self-assembled monolayers," *Langmuir* **20**(17), 7223–7231 (2004).
17. Y. Nakayama et al., "Photocontrol of cell adhesion and proliferation by a photoinduced cationic polymer surface," *Photochem. Photobiol.* **77**(5), 480–486 (2003).
18. J. Edahiro et al., "In situ control of cell adhesion using photoresponsive culture surface," *Biomacromolecules* **6**(2), 970–974 (2005).
19. S. J. Todd et al., "Enzyme activated RGD ligands on functionalized poly(ethylene glycol) monolayers: surface analysis and cellular response," *Langmuir* **25**(13), 7533–7539 (2009).
20. M. Heskins and J. E. Guillet, "Solution properties of poly(N-isopropylacrylamide)," *J. Macromol. Sci. Chem.* **2**(8), 1441–1445 (1968).
21. N. Yamada et al., "Thermo-responsive polymeric surfaces; control of attachment and detachment of cultured cells," *Macromol. Chem. Rapid. Commun.* **11**(11), 571–576 (1990).
22. Y. Tsuda et al., "The use of patterned dual thermoresponsive surfaces for the collective recovery as co-cultured cell sheets," *Biomaterials* **26**(14), 1885–1893 (2005).
23. G. Pasparakis et al., "Laser-induced cell detachment and patterning with photodegradable polymer substrates," *Angew. Chem., Int. Ed.* **50**(18), 4142–4145 (2011).
24. T. Kaji et al., "Nondestructive micropatterning of living animal cells using focused femtosecond laser-induced impulsive force," *Appl. Phys. Lett.* **91**(2), 023904 (2007).
25. H. Moriguchi et al., "An agar-microchamber cell-cultivation system: flexible change of microchamber shapes during cultivation by photo-thermal etching," *Lab. Chip* **2**(2), 125–132 (2002).
26. K. Fukudome et al., "Undesirable contamination of DNA electrophoresed through polyacrylamide and agarose gels as revealed by reversing-pulse electric birefringence signals," *Biopolymers* **31**(12), 1455–1458 (1991).
27. K. Okano et al., "Induction of cell-cell connections by using *in situ* laser lithography on a perfluoroalkyl-coated cultivation platform," *Chembiochem* **12**(5), 795–801 (2011).
28. H. Yamamoto et al., "In-situ guidance of individual neuronal processes by wet femtosecond-laser processing of self-assembled monolayer," *Appl. Phys. Lett.* **99**(16), 163701 (2011).
29. T. Y. Buryakina et al., "Metabolism of HeLa cells revealed through auto-fluorescence lifetime upon infection with enterohemorrhagic," *J. Biomed. Opt.* **17**(10), 101503 (2012).
30. A. Tatiana et al., "Laser-induced cell detachment, patterning, and regrowth on gold nanoparticle functionalized surfaces," *ACS Nano* **6**(11), 9585–9595 (2012).
31. A. G. Doukas and T. J. Flotte, "Physical characteristics and biological effects of laser-induced stress waves," *Ultrasound Med. Biol.* **22**(2), 151–164 (1996).
32. K. Konig et al., "Pulse-length dependence of cellular response to intense near-infrared laser pulses in multiphoton microscopes," *Opt. Lett.* **24**(2), 113–115 (1999).
33. I. H. Chen et al., "Wavelength dependent damage in biological multiphoton confocal microscopy: a micro-spectroscopic comparison between femtosecond Ti:sapphire and Cr:forsterite laser sources," *Opt. Quant. Electron.* **34**(12), 1251–1266 (2002).
34. A. Schonle and S. W. Hell, "Heating by absorption in the focus of an objective lens," *Opt. Lett.* **23**(5), 325–327 (1998).
35. C. J. Weijer, "Collective cell migration in development," *J. Cell Sci.* **122**(18), 3215–3223 (2009).
36. R. Keller, "Shaping the vertebrate body plan by polarized embryonic cell movements," *Science* **298**(5600), 1950–1954 (2002).
37. R. Farooqui and G. Fenteany, "Multiple rows of cells behind an epithelial wound edge extend cryptic lamellipodia to collectively drive cell-sheet movement," *J. Cell Sci.* **118**(1), 51–63 (2005).
38. P. Friedl et al., "Migration of coordinated cell clusters in mesenchymal and epithelial cancer explants in vitro," *Cancer Res.* **55**(20), 4557–4560 (1995).
39. T. Tsuji et al., "Epithelial-mesenchymal transition and cell cooperativity in metastasis," *Cancer Res.* **69**(18), 7135–7139 (2009).
40. S. R. K. Vedula et al., "Emerging modes of collective cell migration induced by geometrical constraints," *Proc. Natl. Acad. Sci. U.S.A.* **109**(32), 12974–12979 (2012).
41. M. K. Driscoll et al., "Cell shape dynamics: from waves to migration," *PLoS Comput. Biol.* **8**(3), e1002392 (2012).
42. K. Koning, "Andrology: effects of ultraviolet exposure and near infrared laser tweezers on human spermatozoa," *Hum. Reprod.* **11**(10), 2162–2164 (1996).
43. Y. Aragane et al., "Ultraviolet light induces apoptosis via direct activation of CD95 (Fas/APO-1) independently of its ligand CD95L," *J. Cell Biol.* **140**(1), 171–182 (1998).
44. J. Nakanishi et al., "Spatiotemporal control of migration of single cells on a photoactivatable cell microarray," *J. Am. Chem. Soc.* **129**(21), 6694–6695 (2007).
45. I. Suzuki et al., "Modification of a neuronal network direction using stepwise photo-thermal etching of an agarose architecture," *J. Nanobiotechnol.* **2**(7), 1–8 (2004).
46. A. K. Vogt et al., "Synaptic plasticity in micropatterned neuronal networks," *Biomaterials* **26**(15), 2549–2557 (2005).
47. N. E. Sanjana and S. B. Fuller, "A fast flexible ink-jet printing method for patterning dissociated neurons in culture," *J. Neurosci. Methods* **136**(2), 151–163 (2004).
48. K. Kato et al., "Immobilized culture of nonadherent cells on an oleyl poly(ethylene glycol) ether-modified surface," *Biotechniques* **35**(5), 1014–1021 (2003).
49. C. E. Helmstetter and S. Cooper, "DNA synthesis during the division cycle of rapidly growing *Escherichia coli*," *J. Mol. Biol.* **31**(3), 507–518 (1968).
50. K. C. Neuman et al., "Characterization of photodamage to *Escherichia coli* in optical traps," *Biophys. J.* **77**(5), 2856–2863 (1999).
51. W. D. Donachie, "Cell length, cell growth and cell division," *Nature* **264**(5584), 328–333 (1976).